The EMBO Journal Vol.17 No.14 pp.3921–3930, 1998

Ca^{2+} binding to synaptotagmin: how many Ca^{2+} ions bind to the tip of a C_2-domain?

Josep Ubach[1,2], Xiangyang Zhang[3], Xuguang Shao[1,2], Thomas C.Südhof[3] and Josep Rizo[1,2,4]

Departments of [1]Biochemistry and [2]Pharmacology, and [3]Department of Molecular Genetics and Howard Hughes Medical Institute, University of Texas Southwestern Medical Center, 5323 Harry Hines Boulevard, Dallas, TX 75235, USA

[4]Corresponding author
e-mail: jose@arnie.swmed.edu

C_2-domains are widespread protein modules with diverse Ca^{2+}-regulatory functions. Although multiple Ca^{2+} ions are known to bind at the tip of several C_2-domains, the exact number of Ca^{2+}-binding sites and their functional relevance are unknown. The first C_2-domain of synaptotagmin I is believed to play a key role in neurotransmitter release via its Ca^{2+}-dependent interactions with syntaxin and phospholipids. We have studied the Ca^{2+}-binding mode of this C_2-domain as a prototypical C_2-domain using NMR spectroscopy and site-directed mutagenesis. The C_2-domain is an elliptical module composed of a β-sandwich with a long axis of 50 Å. Our results reveal that the C_2-domain binds three Ca^{2+} ions in a tight cluster spanning only 6 Å at the tip of the module. The Ca^{2+}-binding region is formed by two loops whose conformation is stabilized by Ca^{2+} binding. Binding involves one serine and five aspartate residues that are conserved in numerous C_2-domains. All three Ca^{2+} ions are required for the interactions of the C_2-domain with syntaxin and phospholipids. These results support an electrostatic switch model for C_2-domain function whereby the β-sheets of the domain provide a fixed scaffold for the Ca^{2+}-binding loops, and whereby interactions with target molecules are triggered by a Ca^{2+}-induced switch in electrostatic potential.

Keywords: C_2-domain/Ca^{2+} binding/protein NMR/synaptotagmin/syntaxin

Introduction

The release of neurotransmitters by synaptic vesicle exocytosis is a tightly regulated process that is triggered by Ca^{2+} influx into presynaptic terminals. A variety of experimental data support the hypothesis that the major Ca^{2+} receptor in this process is the synaptic vesicle protein synaptotagmin I (Südhof, 1995; Südhof and Rizo, 1996). Synaptotagmin I binds phospholipids in a Ca^{2+}-dependent manner with a cooperativity and divalent cation selectivity that correlate with those observed in neurotransmitter release (Brose *et al*., 1992). Synaptotagmin I also interacts with the plasma membrane proteins syntaxin (Bennett *et al*., 1992; Yoshida *et al*., 1992) and neurexins (Petrenko *et al*., 1991; Hata *et al*., 1993). Syntaxin is widely believed to play a key role in exocytosis (Scheller, 1995; Südhof, 1995), while the neurexins include one of the receptors for α-latrotoxin, a toxin that causes massive neurotransmitter release. Electrophysiological experiments in synaptotagmin I knockout mice have demonstrated that this protein is essential for the fast component of neurotransmitter release (Geppert *et al*., 1994). A function for synaptotagmin in this process was supported by analyses of synaptotagmin mutants of *Drosophila melanogaster* and *Caenorhabditis elegans* (Littleton *et al*., 1993; Nonet *et al*., 1993; DiAntonio and Schwartz, 1994), and by microinjection experiments in neural cells (Bommert *et al*., 1993; Elferink *et al*., 1993).

Most of the cytoplasmic region of synaptotagmin I is composed of two consecutive repeats homologous to the C_2-domain of protein kinase C (PKC) (Perin *et al*., 1990, 1991a,b). The isolated first C_2-domain of synaptotagmin I (C_2A-domain) binds phospholipids in a Ca^{2+}-dependent manner similarly to full-length synaptotagmin I (Davletov and Südhof, 1993). The C_2A-domain also exhibits Ca^{2+}-dependent binding to syntaxin (Li *et al*., 1995; Kee and Scheller, 1996; Shao *et al*., 1997a); the Ca^{2+} concentrations required for this interaction parallel those that trigger neurotransmitter release. Thus, this C_2-domain is critical for the function of synaptotagmin I, and elucidating its Ca^{2+}-binding mode and the mechanisms of its Ca^{2+}-dependent interactions is essential for a full understanding of how synaptotagmin I regulates neurotransmitter release.

Identifying the number and nature of Ca^{2+}-binding sites in C_2-domains is of general interest because these protein modules are widespread in nature, and because the functions of many C_2-domains are regulated by Ca^{2+} (Nalefski and Falke, 1996; Rizo and Südhof, 1998). The C_2A-domain of synaptotagmin I and the C_2-domains of phospholipase δ1 (PLC-δ1) and $cPLA_2$ have a very similar β-sandwich structure formed by two four-stranded β-sheets (Sutton *et al*., 1995; Essen *et al*., 1996, 1997; Grobler *et al*., 1996; Shao *et al*., 1996; Perisic *et al*., 1998). Ca^{2+} binding occurs in a region formed by three loops at the top of the C_2-domains, but the exact Ca^{2+}-binding modes are unclear. X-ray diffraction analysis of the C_2A-domain (Sutton *et al*., 1995) revealed a Ca^{2+}-binding site that was formed by four aspartate side chains (which we will refer to as site Ca1). Using NMR spectroscopy, we showed that at least two Ca^{2+} ions bind to the C_2A-domain and revealed a second Ca^{2+}-binding site (Ca2) proximal to the first site (Shao *et al*., 1996). Binding of two Ca^{2+} ions was also observed in crystals of the C_2-domains of PLC-δ1 (Essen *et al*., 1997) and $cPLA_2$ (Perisic *et al*., 1998) but occurred at site Ca1 and a new proximal site (Ca4). This finding led to the suggestion that the C_2A-domain of synaptotagmin I may bind a third Ca^{2+} ion at site Ca4. In addition, it was suggested that

Ca^{2+} may also bind to site Ca2 in the PLC-δ1 C_2-domain since this site was occupied in the La^{3+} complex of this protein (Essen *et al*., 1997). An analogous ternary Ca^{2+}-binding mode has been proposed for the C_2-domain of perforin based on sequence comparisons with PLC-δ1 and synaptotagmin I (Uellner *et al*., 1997).

The results summarized above indicate that the C_2-domains studied bind at least two Ca^{2+} ions in a cluster at the tip of their β-sandwich structure. However, it is still unclear what the complete Ca^{2+}-binding modes of the synaptotagmin I and PLC-δ1 C_2-domains are and how general these binding modes may be. Paraphrasing the medieval question of 'how many angels fit at the tip of a needle?', one might ask: 'how many Ca^{2+} ions bind at the tip of a C_2-domain?'. Answering this question by X-ray diffraction has been difficult because of the low Ca^{2+} affinities of C_2-domains in the absence of ternary agents such as phospholipids, and because of the fragility of the corresponding crystals at high Ca^{2+} concentrations. Taking advantage of the fact that high Ca^{2+} concentrations can be easily achieved in solution to detect weak binding sites, we have now determined the complete Ca^{2+}-binding mode of the C_2A-domain of synaptotagmin I using a combination of Mn^{2+}-induced relaxation experiments, site-directed mutagenesis and Ca^{2+} titrations monitored by NMR spectroscopy. We show that the C_2A-domain contains a novel ternary Ca^{2+}-binding motif that involves sites Ca1, Ca2 and a third proximal site (Ca3). Binding of all three Ca^{2+} ions is required for interaction of the C_2A-domain with syntaxin and is thus likely to be essential for the function of synaptotagmin I in neurotransmitter release.

Results

Mn^{2+}-induced relaxation of amide protons in the C_2A-domain reveals a novel metal-binding site

Changes in the NMR spectra of a protein upon addition of Ca^{2+} can be used to detect Ca^{2+} binding to the protein and define approximately its Ca^{2+}-binding region. However, such changes do not carry strict distance information to determine accurately the locations of Ca^{2+}-binding sites. Such information can be obtained from the strong relaxation effects produced by paramagnetic Ca^{2+} analogs such as Mn^{2+} on nuclei in their proximity (Mildvan and Cohn, 1970). Mn^{2+} causes changes in the CD spectrum and the denaturation temperature of the C_2A-domain of synaptotagmin I that are analogous to those induced by Ca^{2+} binding (Shao *et al*., 1997a; data not shown). Thus, the C_2A-domain appears to bind Mn^{2+} and Ca^{2+} in the same manner. To analyze the Mn^{2+}-binding sites of the C_2A-domain, we used ^1H–^{15}N heteronuclear single quantum correlation (HSQC) spectra. These spectra contain one cross-peak for each amide group in the molecule (except those involving prolines) and thus provide multiple probes to locate Mn^{2+}-binding sites. Since the increase in the relaxation rate of a protein amide proton induced by a bound Mn^{2+} ion is proportional to r^{-6} (where r is the distance between the amide proton and the Mn^{2+} ion), we explored the possibility of establishing correlations between r^{-6} and Mn^{2+}-induced changes in the inverse of ^1H–^{15}N HSQC cross-peak intensities (Δi^{-1}) (see Materials and methods). The amide–metal ion distances used in such correlations were obtained from our calculations of the solution structure of the C_2A-domain (X.Shao, I.Fernandez, T.C.Sudhof and J.Rizo, submitted); Ca^{2+} ions were included in these calculations based on the results described here.

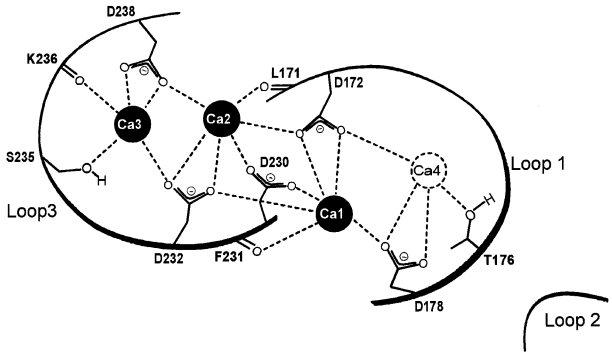

Fig. 1. Ca^{2+}-binding mode of the C_2A-domain. The diagram summarizes the three Ca^{2+}-binding sites observed in the C_2A-domain (Ca1–Ca3, solid circles) and the ligands that participate in each site. The loops that form the Ca^{2+}-binding region (loops 1–3) are also labeled. The results described indicate that a potential fourth site (Ca4, open dotted circle) does not bind Ca^{2+}. The specific ligands were deduced from the experiments described here and from the solution structure of the C_2A-domain (X.Shao, I.Fernandez, T.C.Sudhof and J.Rizo, submitted).

We first recorded a series of ^1H–^{15}N HSQC spectra of the Ca^{2+}-free C_2A-domain (0.6 mM) in the presence of increasing concentrations of Mn^{2+} (0–50 μM). Sub-stoichiometric concentrations of Mn^{2+} were necessary to avoid broadening of the signals of interest beyond detection, and to ensure that chemical exchange effects were minimal. Significant changes in cross-peak intensities were observed at Mn^{2+} concentrations >10 μM. Such changes were restricted to cross-peaks corresponding to amide groups from the Ca^{2+}-binding region, which is formed by the top loops of the C_2A-domain (loops 1–3 in Figure 1) (Sutton *et al*., 1995; Shao *et al*., 1996). Note for instance that, in the expansions displayed in Figure 2, only the cross-peaks corresponding to D178 HN and D238 HN exhibit significant broadening.

The strongest broadening effects at 10 and 20 μM Mn^{2+} corresponded to amide groups close to the site Ca1 (Figure 1) which originally had been identified by X-ray crystallography. Thus, this site is the most populated under these conditions. A logarithmic plot of Δi^{-1} versus HN–Ca1 distances for the data obtained at 20 μM Mn^{2+} (Figure 3A) shows a clear correlation with negative slope that proves this conclusion. As shown in Figure 3B, no such correlation was observed with the distances between the amide protons and the second Ca^{2+}-binding site that we had identified previously by NMR spectroscopy (site Ca2 in Figure 1). These results indicate that little or no binding to this site occurs at 20 μM Mn^{2+}. However, the logarithmic plot of Δi^{-1} at 50 μM Mn^{2+} versus HN–Ca1 distances (Figure 3C) revealed that the $\log(\Delta i^{-1})$ for the two amide protons closest to site Ca2 (D172 HN and D238 HN) deviated from the linear relationship observed for the remaining amide protons, reflecting larger relaxation effects than expected from such a relationship. These results suggest that at 50 μM Mn^{2+} site Ca1 is still the most populated but site Ca2 starts being occupied. ^1H–^{15}N HSQC experiments of the Ca^{2+}-free C_2A-domain

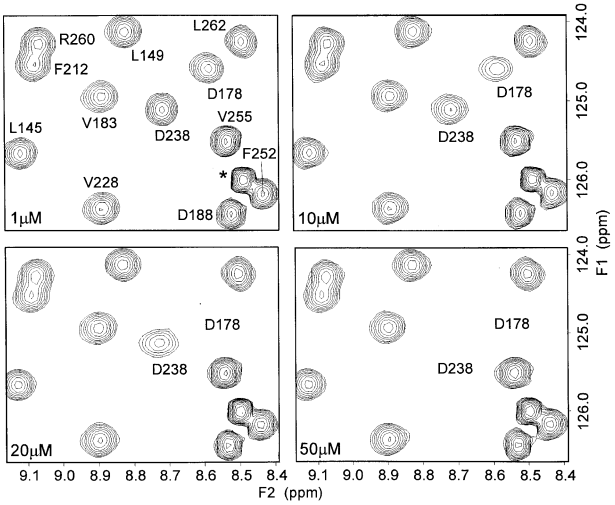

Fig. 2. Mn^{2+}-induced relaxation effects in the ^1H–^{15}N HSQC spectrum of Ca^{2+}-free C_2A-domain. Expansions of ^1H–^{15}N HSQC spectra of 0.6 mM C_2A-domain in the presence 1–50 μM Mn^{2+} (indicated in the lower left corners) are shown. Note that only the cross-peaks corresponding to D178 HN and D238 HN decrease in intensity as a function Mn^{2+} concentration. The remaining cross-peaks in this expansion (only labeled in the upper left plot) are not affected by Mn^{2+} binding to the C_2A-domain.

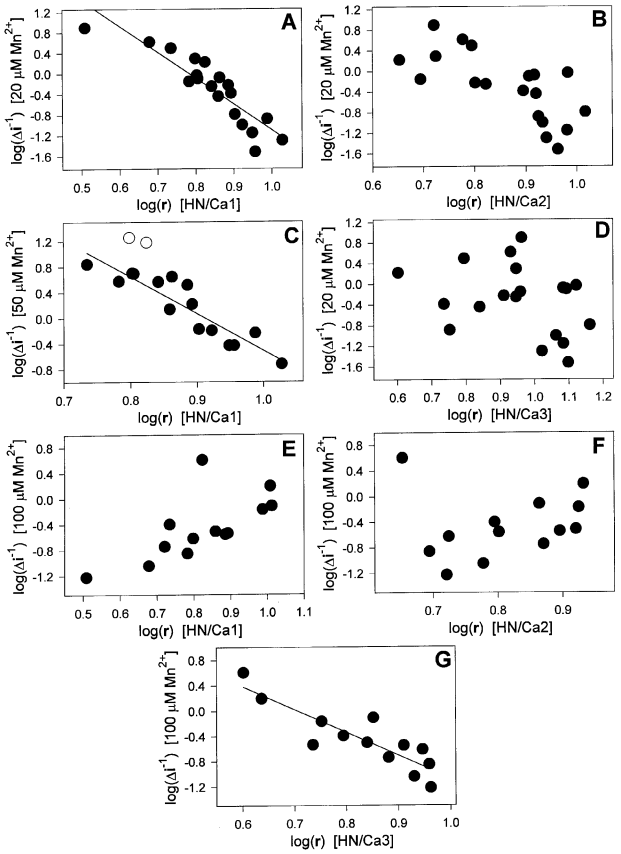

Fig. 3. Correlations between Mn^{2+}-induced effects on ^1H–^{15}N HSQC cross-peaks and distances between amide protons and metal-binding sites. Logarithmic plots of the changes in the inverted intensities of ^1H–^{15}N HSQC cross-peaks induced by Mn^{2+} versus amide proton/metal-binding site distances are shown. Note that both axes in all plots are unitless; within brackets we have indicated on the *y*-axis the Mn^{2+} concentrations used for intensity measurements, and on the *x*-axis the metal-binding sites used to calculate distances to amide protons. The distances were calculated from the solution structure of the C_2A-domain (X.Shao, I.Fernandez, T.C.Sudhof and J.Rizo, submitted). (**A**–**D**) Experiments obtained in the absence of Ca^{2+} which reflect data derived from the cross-peaks of residues 171–178, 180, 200, 201, 230–232, 234, 235, 237, 238 and 240 [the data for the D178 HN cross-peak is not included in (C) because it broadens beyond detection at 50 μM Mn^{2+}]. (**E**–**G**) Experiments performed in the presence of 20 mM Ca^{2+} which reflect data from the cross-peaks of residues 171, 172, 178 and 230–239. The lines in (A), (C) and (G) were calculated by linear regression using the data indicated by solid circles [the data for D172 HN and D238 HN in panel C (○) was not included in the regression].

at concentrations of Mn^{2+} >50 μM resulted in broadening beyond detection of most cross-peaks of interest.

To obtain additional evidence for binding to site Ca2, or potentially other sites, we acquired ^1H–^{15}N HSQC experiments adding Mn^{2+} after saturating the C_2A-domain with 20 mM Ca^{2+}. In principle, if the Mn^{2+} affinities for all sites are identical to the corresponding Ca^{2+} affinities, the populations of Mn^{2+} in each of the sites should be identical in these experiments. However, differences in the relative affinities of Mn^{2+} versus Ca^{2+} among the sites due to the distinct preferred geometries of coordination of the two ions could result in preferential occupation of one of the sites by Mn^{2+} with respect to the others. Significant cross-peak broadening was only observed in these experiments at Mn^{2+} concentrations >50 μM due to the competition of Ca^{2+} for the sites. Logarithmic plots of Δi^{-1} at 100 μM Mn^{2+} versus either HN–Ca1 or HN–Ca2 distances showed no correlation (Figure 3E and F), indicating that the two sites are not populated predominantly by Mn^{2+} under these conditions. Analysis of the cross-peaks exhibiting the strongest broadening effects showed that all the corresponding amide protons were located near a cavity in the structure formed by the side chains of D232, D238 and S235. Hence, these side chains form a third metal-binding site that had not been observed previously (site Ca3 in Figure 1). Logarithmic plots of Δi^{-1} versus HN–Ca3 distances revealed a clear correlation (Figure 3G). Site Ca3 was not significantly populated in the initial experiments performed in the absence of Ca^{2+}, since no correlation was observed in a logarithmic plot of Δi^{-1} at 20 μM Mn^{2+} versus HN–Ca3 distances (Figure 3D), and no broadening above that expected from occupation of site Ca1 and partial occupation of site Ca2 was observed at 50 μM Mn^{2+} for amide protons that are closer to site Ca3 than to sites Ca1 and Ca2.

To explore the possibility that additional metal ions may bind to the C_2A-domain, we searched for sites with high density of potential ligands throughout the surface formed by loops 1–3. We found only a single possible fourth site at a cavity formed by the side chains of D172, T176 and D178, which is in a similar location to the site Ca4 present in the C_2-domains of PLC-δ1 (Essen *et al.*, 1997) and $cPLA_2$ (Perisic *et al.*, 1998). However, comparison of Ca4–HN distances with Mn^{2+}-induced relaxation effects on ^1H–^{15}N HSQC spectra indicated that this site is not significantly populated. We acquired a series of TOCSY spectra under conditions analogous to those used for the ^1H–^{15}N HSQC spectra to monitor Mn^{2+}-induced broadening effects on Hα and side chain protons that might indicate binding to site Ca4, but no such binding was observed (data not shown). Mn^{2+}-induced broadening outside the region formed by loops 1–3 was only observed

for protons of the D150–Y151–D152 sequence in the ^{1}H–^{15}N HSQC and TOCSY spectra acquired in the presence of 20 mM Ca^{2+}. However, protons of this sequence only exhibit very minor Ca^{2+}-induced chemical shift changes (Shao *et al*., 1996, 1997b) that occur at 20 mM Ca^{2+} concentrations, excluding the possibility that this represents a specific Ca^{2+}-binding site.

Mn^{2+}-induced relaxation effects on ^{1}H–^{15}N HSQC spectra have been used in qualitative analyses of Mn^{2+}-binding sites in proteins (Lin *et al*., 1996), but to our knowledge they have not been used previously in a quantitative manner. The correlations between changes in ^{1}H–^{15}N HSQC cross-peak intensities and Mn^{2+}–amide proton distances shown here (Figure 3A and G) indicate that this simple method could be used to derive distance restraints that could be included in protein structure calculations. Indeed, the Mn^{2+}–HN distances that can be calculated from these correlations using one of the distances as a reference fall in general within <1 Å from the Ca1–HN and Ca3–HN distances observed in the solution structure of the C_2A-domain (X.Shao, I.Fernandez, T.C.Sudhof and J.Rizo, submitted), and from the Ca1–HN distances observed by X-ray crystallography (Sutton *et al*., 1995). The method is expected to yield even better results for proteins with single metal-binding sites or multiple more separated sites.

Ca^{2+} titrations of wild-type and mutant C_2A-domains demonstrate a ternary Ca^{2+}-binding motif

The Mn^{2+}-induced broadening effects demonstrated the presence of two Mn^{2+}-binding sites in the C_2A-domain (Ca1 and Ca3) and provided evidence for the existence of an Mn^{2+}-binding site (Ca2) with an affinity lower than that of Ca1 and higher than that of Ca3. To investigate whether Ca^{2+} binds to these and possibly other sites, we performed Ca^{2+} titrations monitored by ^{1}H–^{15}N HSQC spectra of the wild-type (WT) C_2A-domain and of C_2A-domains containing point mutations designed to eliminate binding to one or more of the potential Ca^{2+}-binding sites. Conservative mutations were used to avoid perturbations of the structure of the C_2A-domain. Thus, some of the aspartate residues that form the binding sites were replaced individually by asparagine (D178N, D232N and D238N mutants), and the serine and threonine implicated in sites Ca3 and Ca4, respectively, were replaced by alanine (S235A and T176A mutants). We also prepared a C_2A-domain containing a mutation of D238 to alanine (D238A mutant). An upgrade of our NMR spectrometer and the use of a sensitivity-enhanced pulse sequence including a water flip-back pulse (Zhang *et al*., 1994) allowed us to acquire ^{1}H–^{15}N HSQC experiments with much higher sensitivity than in our previous titration of the WT C_2A-domain (Shao *et al*., 1996) and to monitor key cross-peaks that previously were broadened beyond detection in the mid-points of the Ca^{2+} titration due to chemical exchange. Three-dimensional (3D) ^{1}H–^{15}N NOESY-HSQC spectra of each mutant C_2A-domain were acquired to assign the ^{1}H–^{15}N HSQC cross-peaks that changed in position with respect to the WT C_2A-domain due to the mutation introduced. The most important observations drawn from the titrations of WT and mutant C_2A-domains are summarized below, using the expansions of Figures 4–6 as examples.

The titration of the WT C_2A-domain demonstrates the presence of three Ca^{2+}-binding components that can be associated with sites Ca1, Ca2 and Ca3 when compared with the components observed in the titrations of the mutant C_2A-domains. All larger changes in amide ^{1}H and ^{15}N chemical shifts caused by Ca^{2+} binding to each site are local, consistent with the fact that Ca^{2+} produces stabilization of the structure of the C_2A-domain rather than a change from a well-defined conformation to another (Shao *et al*., 1996). Thus, the proximities of amide groups to each site can be used qualitatively to rationalize the components observed for many of the cross-peaks in terms of sequential binding to sites Ca1, Ca2 and Ca3.

The behavior of the ^{1}H–^{15}N HSQC cross-peak corresponding to D238 HN (Figure 4A–D) provides one of the best examples to illustrate the sequential binding. This amide group is sufficiently close to all three sites (within 7 Å or less) to exhibit substantial changes associated with Ca^{2+} binding to each site. Thus, three components are clearly distinguishable along the titration of the WT C_2A-domain (Figure 4A). The S235A mutation, which is predicted to abolish Ca^{2+} binding to the Ca3 site, causes loss of the lowest affinity component (Figure 4B). Only the highest affinity component is unaffected after the D238A mutation (Figure 4C), which is predicted to disrupt Ca^{2+} binding to sites Ca2 and Ca3. The only large Ca^{2+}-induced chemical shift changes that remain in the titration of the D238A mutant correspond to HN groups close to site Ca1 such as that of T176 (Figure 5A and B), showing that the highest affinity component corresponds to binding to this site. As expected, these large changes are not observed for the D178N mutant in which binding to site Ca1 is disrupted (Figure 5C). The cross-peak corresponding to S235 HN provides another example of triphasic behavior during the titration of the WT C_2A-domain (Figure 6A). This amide group is very close to sites Ca2 and Ca3 but farther from site Ca1. Correspondingly, the highest affinity component is associated with small chemical shift changes, while binding to sites Ca2 and Ca3 causes much larger changes. These larger changes are not observed after disrupting binding to these sites with the D238A mutation (Figure 6B). The results obtained for the D232N mutant were similar to those obtained for the D238A mutant, showing that either the D232 side chain is not essential for Ca^{2+} binding to site Ca1 or that asparagine can act as a ligand for this site.

Mutations in loop 3 (D232N, S235A and D238A) abolished the expected titration components but had only small effects on the chemical shift changes caused by Ca^{2+} binding to the remaining site(s) (e.g. compare Figure 4B and C with A, and Figure 6B with A). The D178N mutation in loop 1 eliminated Ca^{2+} binding to site Ca1, as expected, but in addition caused widespread perturbations of the chemical shifts in the Ca^{2+}-binding region, decreased Ca^{2+} affinities for sites Ca2 and Ca3, and changes in the way Ca^{2+} binding to these two sites affects cross-peak movement (compare Figure 4D with A). The D178 side chain is in a compact region of the molecule, in close proximity to the R199 and K200 side chains and forming a hydrogen bond with K200 HN. Thus, the D178N mutation may perturb the electrostatic balance in

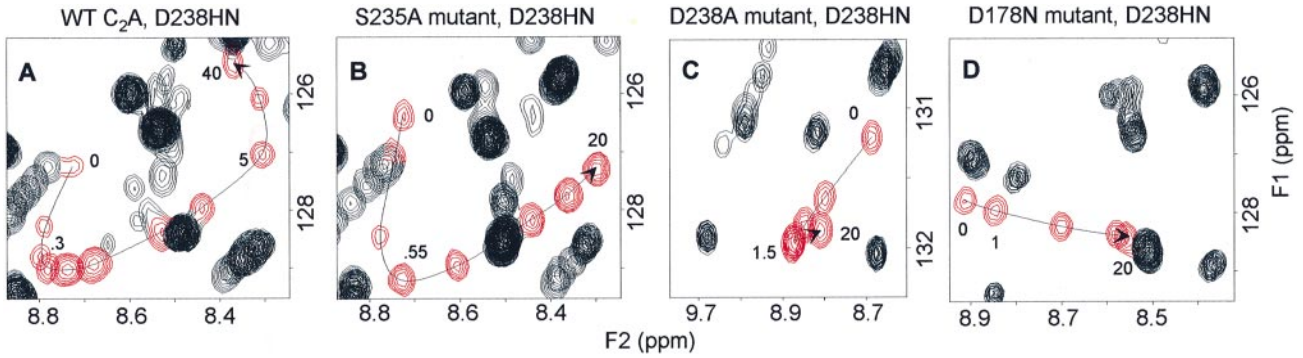

Fig. 4. Ca^{2+} titrations of WT and mutant C_2A-domains monitored by ^1H–^{15}N HSQC spectra. The plots represent superpositions of expansions of ^1H–^{15}N HSQC spectra that illustrate the movements of the cross-peaks discussed in the text (red contours) as a function of Ca^{2+} concentration. The C_2A-domain corresponding to each expansion and the HN cross-peak monitored are indicated above each plot. Only a subset of the ^1H–^{15}N HSQC spectra acquired for each titration is shown. The total Ca^{2+} concentrations used for each superimposed spectrum in millimolar units were (some are indicated next to the red cross-peaks): (**A**) 0, 0.1, 0.2, 0.3, 0.45, 0.6, 1.2, 2, 5, 20, 40; (**B**) 0, 0.075, 0.25, 0.55, 1, 3, 6, 20; (**C**) 0, 0.2, 0.4, 0.8, 1.5, 20; and (**D**) 0, 1, 5, 15, 20.

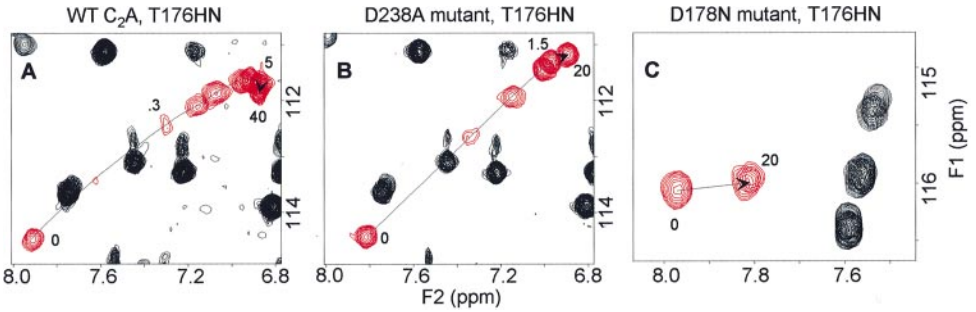

Fig. 5. Ca^{2+} titrations of WT and mutant C_2A-domains monitored by ^1H–^{15}N HSQC spectra. The expansions correspond to the same experiments described in Figure 4. The total Ca^{2+} concentrations used (mM) were: (**A**) 0, 0.1, 0.3, 0.45, 0.6, 1.2, 2, 5, 40; (**B**) 0, 0.2, 0.4, 0.8, 1.5, 20; and (**C**) 0, 15, 20.

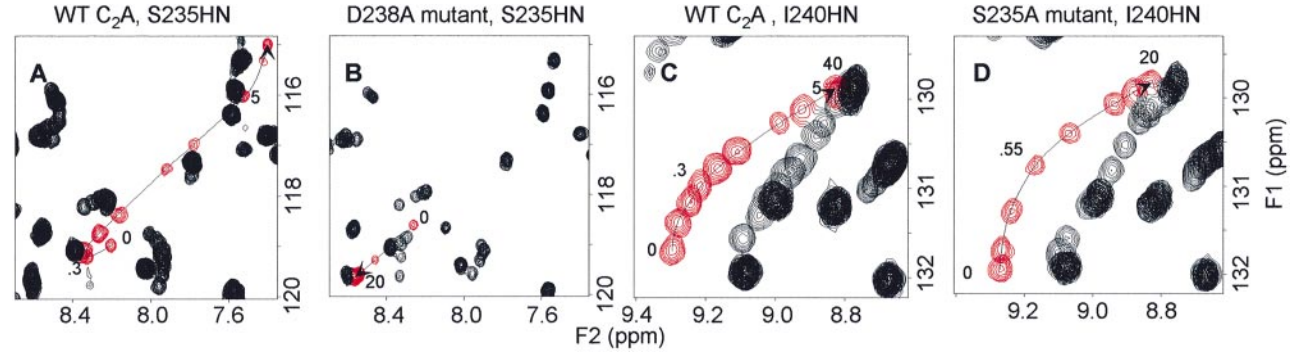

Fig. 6. Ca^{2+} titrations of WT and mutant C_2A-domains monitored by ^1H–^{15}N HSQC spectra. The expansions correspond to the same experiments described in Figure 4. The total Ca^{2+} concentrations used (mM) were: (**A**) 0, 0.1, 0.2, 0.3, 0.45, 0.6, 1.2, 2, 5, 20, 40; (**B**) 0, 0.075, 0.25, 0.55, 1, 3, 6, 20; (**C**) 0, 0.1, 0.2, 0.3, 0.45, 0.6, 1.2, 2, 5, 40; and (**D**) 0, 0.075, 0.25, 0.55, 1, 3, 6, 20.

the region and the structure of the Ca^{2+}-binding loops, which may affect binding to sites Ca2 and Ca3. It is also likely that Ca^{2+} binding to site Ca1 in the WT C_2A-domain, which occurs with the highest affinity among the three sites, makes a major contribution to the Ca^{2+}-induced structural stabilization of the C_2A-domain and helps bring the side chains of D172, D230 and D232 into the orientations required for the formation of sites Ca2 and Ca3.

In the titration of the D238N mutant, a very low affinity component was observed in addition to the component associated with binding to site Ca1 (data not shown). The D238A mutant was prepared to eliminate the possibility that this low affinity component could be due to residual binding of Ca^{2+} to site Ca2 or Ca3 since asparagine could still act as a Ca^{2+} ligand; however, the component remained even after the Asp to Ala mutation (e.g. Figure 4C). It is likely that removing the D238 side chain is not sufficient to abolish completely Ca^{2+} binding to site Ca2 since the directions of cross-peak movements associated with this very low affinity component are similar to those caused by binding to site Ca2 in the WT C_2A-domain. This conclusion is supported by the observation that this residual component was not present in the titration of the D232N mutant, where Ca^{2+} binding to site Ca2 should be completely abolished since the D232 side chain contributes

two ligands to this site (Figure 1). A possible explanation for the very low affinity component could also be that a fourth Ca^{2+} ion binds to the putative Ca4 site. However, a Ca^{2+} titration of the C_2A-domain containing the T176A mutation, which should disrupt this potential site, yielded cross-peak titration curves that were very similar to those of the WT C_2A-domain (data not shown). We also performed titrations of the WT C_2A-domain monitored by TOCSY spectra to investigate whether chemical shift changes in side chains near site Ca4 would reveal binding to this site. These titrations again exhibited three components that can be associated with binding to sites Ca1–Ca3 but gave no evidence of binding to site Ca4.

Calculation of Ca^{2+} affinities for sites Ca1–Ca3 from the Ca^{2+} titration of the WT C_2A-domain is most reliable using the titration curves of chemical shifts that experience large changes from binding to one site and small changes from binding to the other sites. The curve for the ^{15}N chemical shift of the K200 HN yielded a K_D for site Ca1 of ~75 μM, similar to the value obtained in our previous titration (60 μM, Shao *et al*., 1996). The titration curve for the ^{1}H chemical shift of the I240 HN, which is affected mainly by binding to site Ca2 (Figure 6C and D), yields a K_D for site Ca2 of ~ 500 μM, also similar to the value obtained previously (400 μM, Shao *et al*., 1996). No HN chemical shift was affected predominantly by binding to site Ca3, but the titration curves for the amide groups of S235 and D238 (Figures 4A and 6A) indicate a K_D of well above 1 mM for the third component. Thus, Ca3 is a very low affinity site.

Binding of three Ca^{2+} ions to the C_2A-domain is required for binding to syntaxin

The Ca^{2+}-dependent interactions of the C_2A-domain of synaptotagmin I with phospholipids (Davletov and Südhof, 1993) and with syntaxin (Li *et al*., 1995) are likely to be critical for its function in neurotransmitter release. A question that arises from the results described above is whether Ca^{2+} binding to all of the three sites (Ca1–Ca3) is required for the function of the C_2A-domain, particularly considering the low Ca^{2+} affinity of site Ca3. To address this question, we studied the Ca^{2+}-dependent binding of the WT and mutant C_2A-domains to syntaxin. The broadening observed in the ^{1}H–^{15}N HSQC cross-peaks of the C_2A-domain upon binding to unlabeled syntaxin or to the unlabeled N-terminal domain of syntaxin (SyxN) provides a sensitive method to detect this interaction (Shao *et al*., 1997a). As shown in Figure 7A and B, addition of 5 mM Ca^{2+} to ^{15}N-labeled C_2A-domain in the presence of unlabeled SyxN caused very severe broadening of the C_2A-domain ^{1}H–^{15}N HSQC cross-peaks. However, no broadening was observed even at 20 mM Ca^{2+} in ^{1}H–^{15}N HSQC spectra of the D178N, D232N, D238A and S235A mutants acquired in the presence of SyxN (Figure 7C–F). Thus, Ca^{2+} binding to all three sites is essential for the interaction of the C_2A-domain with syntaxin. On the other hand, the T176A mutant exhibited a very similar behavior to that of WT in analogous experiments (Figure 7G and H), showing that even if the potential Ca4 site exists, Ca^{2+} binding to this site is not required for Ca^{2+}-dependent binding to syntaxin. These results correlate with those of parallel experiments which showed that Ca^{2+} binding to sites Ca1, Ca2 and Ca3 but not to site Ca4 is required for binding of the C_2A-domain to phospholipids (Zhang *et al*., 1998).

Discussion

Synaptic vesicle exocytosis is regulated by a cascade of protein–protein interactions that mediate targeting of the vesicles to the plasma membrane (docking), preparation of the vesicles for fusion (priming) and membrane fusion upon Ca^{2+} influx into the presynaptic terminals (Südhof, 1995). Synaptotagmin I is essential for neurotransmitter release (Geppert *et al*., 1994) and is believed to be the main Ca^{2+} receptor in this process (Südhof and Rizo, 1996). The C_2A-domain, through its Ca^{2+}-dependent interactions with phospholipids and syntaxin, is likely to be critical for the role of synaptotagmin in evoked exocytosis. Elucidation of the Ca^{2+}-binding mode of the C_2A-domain is thus a necessary step toward understanding this role.

Building on previous studies, here we have now shown that the C_2A-domain binds three Ca^{2+} ions in a cluster formed by one serine and five aspartate side chains. These results were incorporated into our calculations of the solution structure of the C_2A-domain (X.Shao, I.Fernandez, T.C.Sudhof and J.Rizo, submitted) to yield the complete Ca^{2+}-binding mode summarized in Figure 1, which also involves three backbone carbonyl groups. Binding of three Ca^{2+} ions by the C_2A-domain correlates with the Hill coefficient of 3.1 observed in Ca^{2+}-dependent phospholipid binding (Davletov and Südhof, 1993) and fits well with an important role for the C_2A-domain in neurotransmitter release since this process is characterized by a high Ca^{2+} cooperativity (Heidelberger *et al*., 1994). Neurotransmitter release is associated with a low affinity Ca^{2+} receptor since it is half-maximal at ~200 μM Ca^{2+} (Heidelberger *et al*., 1994). While this Ca^{2+} requirement is close to the dissociation constants of sites Ca1 and Ca2 (~60–75 and ~400–500 μM, respectively), it could be argued that site Ca3 is not biologically relevant since it has a very low affinity ($K_D >> 1$ mM). However, Ca^{2+} binding to site Ca3 causes large and specific chemical shift changes and is required for the interaction of the C_2A-domain with phospholipids and syntaxin. Thus, site Ca3 is most likely as important as the other two sites for the function of the C_2A-domain.

The low affinites of the three Ca^{2+}-binding sites of the C_2A-domain could be due to the fact that they have incomplete coordination spheres, particularly site Ca3 which has only five ligands (Figure 1). Such incomplete coordination may be important for C_2A-domain function since the empty sites may be occupied by phosphate groups in lipid interactions and by acidic side chains in the interaction with syntaxin. This hypothesis is supported by the observation that Ca^{2+}-dependent phospholipid binding occurs with much higher apparent Ca^{2+} affinity (~5 μM, Davletov and Südhof, 1993). Ca^{2+}-dependent binding to syntaxin is half-maximal at ⩾200 μM Ca^{2+} (Li *et al*., 1995) and hence it does not produce such a dramatic increase in the apparent Ca^{2+} affinity of the C_2A-domain. However, the largest chemical shift changes in the C_2A-domain caused by Ca^{2+}-dependent binding to syntaxin are observed at the region around sites Ca2 and Ca3 (Shao *et al*., 1997a), in favor of the proposal that

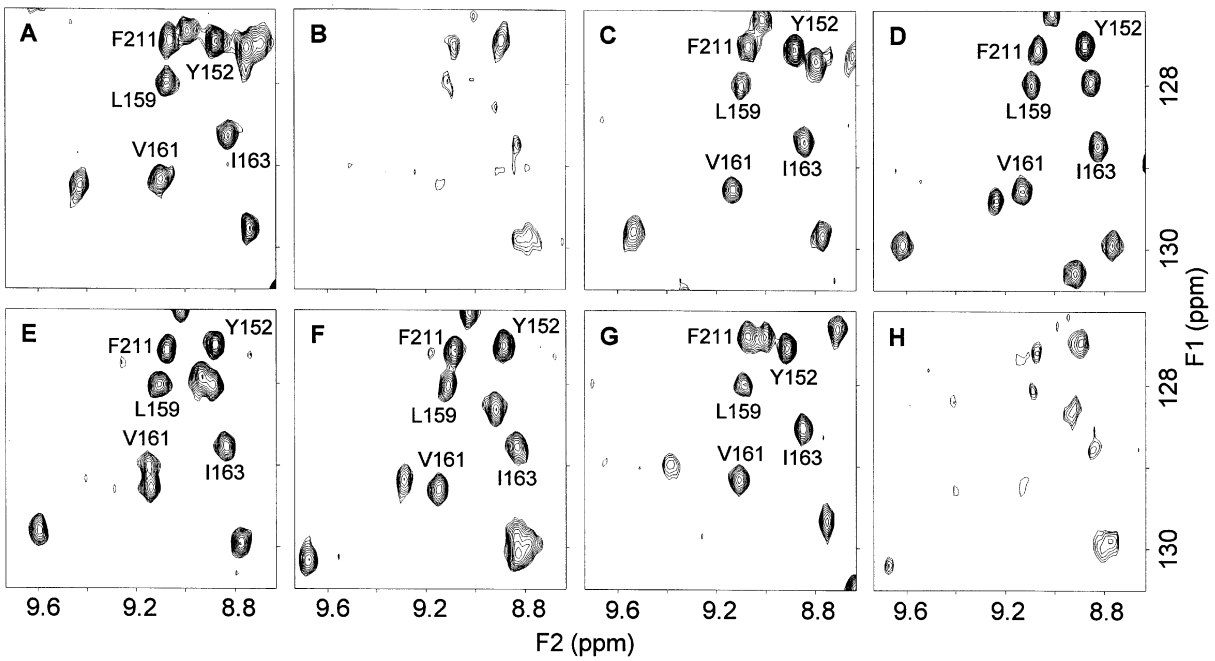

Fig. 7. Binding of all three Ca^{2+} ions is required for the interaction of the C_2A-domain with syntaxin. Expansions of ^1H–^{15}N HSQC spectra of 100 μM ^{15}N-labeled WT and mutant C_2A-domains in the presence of 100 μM syntaxin N-terminal domain and different Ca^{2+} concentrations are shown. The expansions correspond to the following C_2A-domain and Ca^{2+} concentrations: (**A**) WT, 0 mM Ca^{2+}; (**B**) WT, 5 mM Ca^{2+}; (**C**) D178N mutant, 20 mM Ca^{2+}; (**D**) D238A mutant, 20 mM Ca^{2+}; (**E**) D232N mutant, 20 mM Ca^{2+}; (**F**) S235A mutant, 20 mM Ca^{2+}; (**G**) T176A mutant, 0 mM Ca^{2+}; and (**H**) T176A mutant, 5 mM Ca^{2+}. The spectra in (C), (D), (E) and (F) do not exhibit any broadening compared with spectra acquired in the absence of Ca^{2+} (not shown). Cross-peaks that are in similar positions in the ^1H–^{15}N HSQC spectra of the WT and mutant C_2A-domains have been labeled in expansions (A) and (C–G).

coordination of these sites by syntaxin side chains contributes to binding.

Analysis of the mechanism of Ca^{2+}-dependent binding of the C_2A-domain to syntaxin showed that the region around the Ca^{2+}-binding sites is responsible for the protein–protein interaction and that binding is likely to be triggered by a change in the electrostatic potential of this region (Shao *et al*., 1997a). These observations led to a model whereby synaptotagmin acts as an electrostatic switch in neurotransmitter release. According to this model, the C_2A-domain is presumed to be close to syntaxin before Ca^{2+} influx, but electrostatic repulsion between the two proteins prevents fusion from proceeding; upon Ca^{2+} influx, Ca^{2+} binding to the C_2A-domain would attract syntaxin, triggering fusion by the exocytotic machinery. The observation that binding of three Ca^{2+} ions to the C_2A-domain is required for syntaxin binding reinforces the electrostatic switch model. Figure 8 shows how sequential binding of Ca^{2+} ions to the C_2A-domain causes a transition from a zwitterionic but mainly negative electrostatic potential to a highly positive potential. Analysis of the mechanism of binding of the C_2A-domain to phospholipids has also shown the importance of electrostatics for this interaction (Zhang *et al*., 1998). A key question is whether the interactions of the C_2A-domain with either syntaxin, phospholipids or both are involved in evoked exocytosis. The finding that both interactions occur by similar mechanisms implies that if both of them are relevant they should occur in a sequential manner. It is tempting to speculate that proximity of the C_2A-domain to syntaxin within the fusion complex could favor this interaction first, when the influx of high Ca^{2+} concentration invades the presynaptic terminal; such proximity could also increase the apparent Ca^{2+} affinity and cooperativity of the C_2A-domain–syntaxin interaction. After Ca^{2+} is diffused away rapidly, the interaction with syntaxin may be lost, but sufficient Ca^{2+} may remain for binding to phospholipids, which may be favored by the approach of the two membranes associated with fusion. The C_2A-domain–membrane interaction may then contribute to facilitate endocytosis.

The approach that we followed to study Ca^{2+} binding to the C_2A-domain is based on simple NMR experiments and may find general application to analyze Ca^{2+}-binding sites of relatively weak affinity in proteins. This methodology has allowed us to answer in part the medieval question set forth in the Introduction: the number of Ca^{2+} ions that bind at the tip of the C_2A-domain of synaptotagmin I is three. While binding of multiple Ca^{2+} ions has been observed previously in proteins with several EF-hand motifs such as calmodulin (Babu *et al*., 1985) or in multidomain proteins such as cadherin (Nagar *et al*., 1996), the ternary Ca^{2+}-binding mode of the C_2A-domain is unique in that the three Ca^{2+} ions bind in close proximity at the tip of a single protein domain (Figure 8E). A similar ternary Ca^{2+}-binding motif to that described here for the C_2A-domain has also been observed in the C_2-domain of PKC-β by X-ray crystallography (B.Sutton and S.Sprang, personal communication). The immediate question that arises is how general this Ca^{2+}-binding mode may be in other C_2-domains? The PLC-δ1 and $cPLA_2$ C_2-domains contain one of the Ca^{2+}-binding sites of the C_2A-domain (site Ca1) and a different site (Ca4) (Essen *et al*., 1997; Perisic *et al*., 1998). The $cPLA_2$ C_2-domain is unlikely to

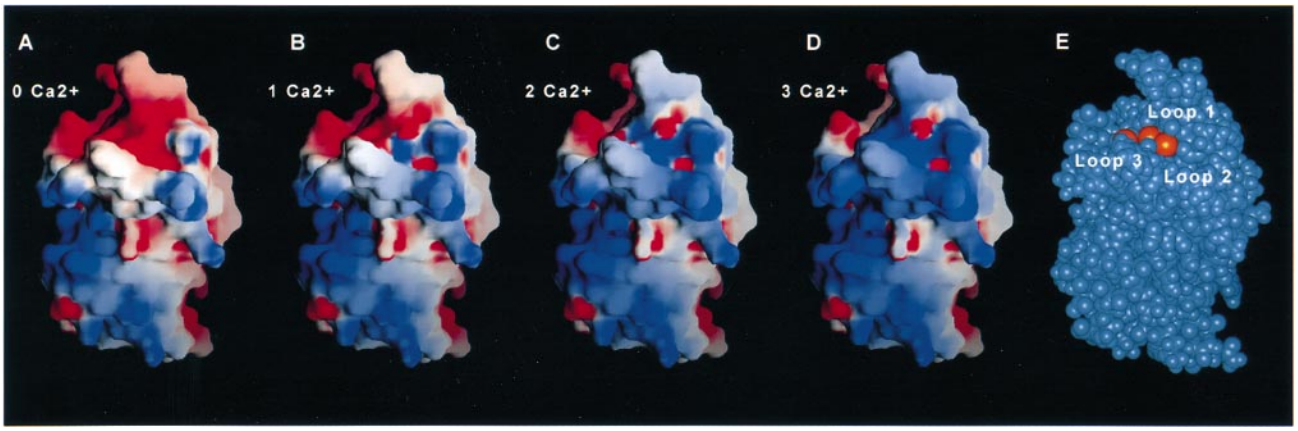

Fig. 8. Change in the electrostatic potential of the C_2A-domain upon progressive binding of Ca^{2+} to sites Ca1, Ca2 and Ca3. (A–D) The surface electrostatic potential of the C_2A-domain in the Ca^{2+}-binding region is shown before Ca^{2+} binding (**A**) and after Ca^{2+} binding to site Ca1 (**B**), to sites Ca1 and Ca2 (**C**) and to sites Ca1, Ca2 and Ca3 (**D**). The surfaces were calculated using the program GRASP (Nicholls *et al*., 1991) and the solution structure of Ca^{2+}-bound C_2A-domain (X.Shao, I.Fernandez, T.C.Sudhof and J.Rizo, submitted) after removing the appropriate Ca^{2+} ions. The gradient of electrostatic potential shown ranges from $\geqslant -7\ k_BT/e$ (red) to $\leqslant 7\ k_BT/e$ (blue). (**E**) Space-filling model of the C_2A-domain (blue) with three bound Ca^{2+} ions (orange), in the same orientation used for (A–D). The model illustrates the unusual nature of C_2-domains, which are designed to bind multiple Ca^{2+} ions in a small region at the tip of their elliptically shaped structure (the largest Ca^{2+}–Ca^{2+} distance is 6 Å while the long diameter of the ellipse is ~50 Å).

contain additional sites since it has been shown to bind only two Ca^{2+} ions by equilibrium dialysis and stopped-flow fluorescence spectroscopy (Nalefski *et al*., 1997). However, the PLC-δ1 C_2-domain binds La^{3+} in the Ca2 site (Essen *et al*., 1997) and contains the side chains that form site Ca3 in the C_2A-domain of synaptotagmin I. Therefore, the PLC-δ1 C_2-domain potentially could bind a total of four Ca^{2+} ions at sites Ca1–Ca4. From sequence alignments of C_2-domains (Brose *et al*., 1995; Nalefski and Falke, 1996), it appears that sites Ca1 and Ca2, which form what we previously named the C_2-motif (Shao *et al*., 1996), may be the most abundant in C_2-domains but sites Ca3 and/or Ca4 may also be present in many C_2-domains. Analysis of additional C_2-domains will be required to evaluate this prediction. The picture that emerges from the available data is that C_2-domains have been designed to project a large number of Ca^{2+}-binding side chains in a small region at the tip of a compact β-sandwich, in such a way that coordination sites remain available in the Ca^{2+} ions for interaction with other molecules. The particular Ca^{2+}-binding sites formed and the side chains in the Ca^{2+}-binding loops provide functional specificity.

Materials and methods

Protein expression and purification

The plasmids encoding GST fusions of the WT and mutant rat C_2A-domains (residues 140–267 of synaptotagmin I) are described elsewhere (Davletov and Südhof, 1993; Zhang *et al*., 1998). The construct to express the GST fusion of the rat syntaxin 1a N-terminal domain (residues 1–180) was obtained by PCR as described (Zhang *et al*., 1998). Soluble proteins were obtained by overexpression of the GST fusions in *Escherichia coli* BL21(DE3), purification by affinity chromatography on glutathione–agarose, thrombin cleavage and final purification by gel filtration or anion exchange chromatography as described (Shao *et al*., 1997a). Uniform ^{15}N labeling was achieved by growing the cells in M9 minimal medium containing $^{15}NH_4Cl$ as the only nitrogen source. Similar yields were obtained for all proteins (~5 mg of pure protein per liter of culture).

NMR spectroscopy

All NMR spectra were acquired on a Varian Unity 500 spectrometer using a triple resonance probe. ^1H–^{15}N 2D HSQC (Bodenhausen and Ruben, 1980) and 3D NOESY-HSQC (Marion *et al*., 1989) spectra were acquired using sensitivity-enhanced pulse sequences incorporationg pulsed-field gradients and a water flip-back pulse (Zhang *et al*., 1994). ^1H–^{15}N HSQC spectra were acquired with spectral widths of 7600 and 1163 Hz in the F2 and F1 dimensions, respectively, and consisted of 2×100 FIDs of 768 complex points each, with 16 scans per FID (1 h total acquisition time). Zero filling, Fourier transformation and removal of the aliphatic part in the F2 dimension yielded matrices of 512×512 real points. In ^1H–^{15}N NOESY-HSQC spectra, the F3, F2 and F1 dimensions had spectral widths of 7600, 1163 and 6000 Hz, respectively, and consisted of 512, 42 and 128 complex points, respectively (eight scans per FID). Linear prediction in the F2 dimension, zero filling, Fourier transformation and removal of the F3 aliphatic region yielded matrices of 512×128×512 real points. TOCSY spectra (Davis and Bax, 1985) consisted of 2×256 FIDs of 1024 complex points, with 16 scans per FID. Zero filling and Fourier transformation led to matrices of 1024×1024 real points. In all spectra, Gaussian apodization was used for the directly acquired dimension and shifted sine bells for the other dimensions. Processing was performed with the program Felix (MSI).

Mn^{2+} relaxation experiments

At the motion regimes characteristic of proteins, the increase in the relaxation rates of protein nuclei caused by bound Mn^{2+} is dominated by dipolar interactions and is thus proportional to r^{-6}, where r is the distance between the protein nucleus and the Mn^{2+} ion (Bloembergen, 1957). Since resonance intensities are inversely proportional to transverse relaxation rates, the difference between the inverted intensities of the nucleus resonance in the presence and absence of Mn^{2+} (Δi^{-1}) can be approximated as a magnitude proportional to r^{-6}, and logarithmic plots of Δi^{-1} versus r^{-6} should be linear with a negative slope. Extension of this concept to a relationship between Mn^{2+}–amide proton distances and ^1H–^{15}N HSQC cross-peak intensities is complicated by the fact that increased longitudinal relaxation rates effectively decouple the ^1H–^{15}N interactions that give rise to the cross-peaks, and increased transverse relaxation rates affect the INEPT and reverse INEPT transfer steps, the linewidths in the F2 dimension and, although to a lesser extent, the F1 linewidths. While changes in proton relaxation times constitute more straightforward parameters to correlate with r, ^1H–^{15}N HSQC cross-peak intensities are very easily measured and thus we explored whether there was a phenomenological correlation between r and changes in such intensities.

C_2A-domain samples for ^1H–^{15}N HSQC spectra to study Mn^{2+}-induced relaxation effects were prepared by extensive dilution and concentration in 40 mM perdeuterated acetate, 100 mM NaCl using H_2O/D_2O 9:1 as the solvent. The pH was adjusted to 5.0 to allow observation of all amide protons. Two sets of ^1H–^{15}N HSQC experiments were acquired at 31°C, one with 0.6 mM C_2A-domain in the absence of Ca^{2+}, with additions of 0, 0.1, 10, 20, 50 and 100 μM $MnCl_2$, and the other with 0.5 mM C_2A-domain in the presence of 20 mM $CaCl_2$, with

additions of 0, 10, 50, 100 and 200 μM $MnCl_2$. TOCSY spectra were acquired under analogous conditions using D_2O as the solvent but the results were only analyzed qualitatively. ^1H–^{15}N HSQC cross-peak intensities were measured with the program Felix (MSI). For each cross-peak at each Mn^{2+} concentration, values of Δi^{-1} were calculated as the difference between the inverse of the cross-peak intensitiy at the given Mn^{2+} concentration and the inverse of the cross-peak intensity in the absence of Mn^{2+} (all intensities normalized by the intensity in the absence of Mn^{2+}). Logarithmic plots of Δi^{-1} values measured at a given Mn^{2+} concentration versus the distance of the corresponding amide proton to a particular metal-binding site were constructed using the program Sigma Plot (Jandel Scientific) and linear regressions were calculated using the same program. Regression coefficients for the data represented in the plots of Figure 3A, C and G and in others obtained at different Mn^{2+} concentrations ranged from 0.84 to 0.92, and the slopes were from –3.7 to –6.5.

Ca^{2+} titrations and syntaxin-binding experiments

Samples for Ca^{2+} titrations were prepared by succesive dilution and concentration in 40 mM Tris–HCl-d_{11} (pH 7.4), 100 mM NaCl, 50 μM EDTA, using H_2O/D_2O 6:1 as the solvent for ^1H–^{15}N HSQC spectra or D_2O for TOCSY spectra. The final free EDTA concentration was estimated from the height of the 3.6 p.p.m. resonance in the 1D ^1H NMR spectrum. Titrations monitored by ^1H–^{15}N HSQC spectra were performed at 25°C for WT and mutant C_2A-domain with 120–150 μM protein concentrations (measured from the maximum absorption at 280 nm). A titration monitored by TOCSY spectra was performed at 25°C with 475 μM WT C_2A-domain. The desired Ca^{2+} concentrations were obtained by addition of 1–3 μl aliquots of $CaCl_2$ solutions prepared from a stock solution of 5 M $CaCl_2$. Given the low Ca^{2+} affinities of the C_2A-domain, free Ca^{2+} concentrations were calculated as the excess of Ca^{2+} over EDTA. Samples to test binding of the C_2A-domain to the N-terminal domain of syntaxin (SyxN, residues 1–180 of syntaxin 1a) were prepared in an analogous manner to that used for the ^1H–^{15}N HSQC Ca^{2+} titrations, and a series of ^1H–^{15}N HSQC experiments with increasing Ca^{2+} concentrations up to 20 mM were acquired at 25°C for the WT and each mutant C_2A-domain (100 μM) in the presence of 100 μM SyxN.

Acknowledgements

We thank Lewis Kay for providing pulse sequences, Imma Fernandez for fruitful discussions, and Bryan Sutton and Steve Sprang for sharing data before publication. J.U. was a fellow from the Direccio General de Recerca, Generalitat de Catalunya, Spain. This work was supported by a joint grant from the William Randolph Hearst Foundation and the United Cerebral Palsy Research and Educational Foundation, and by NIH grant NS33731 (to J.R.).

References

Babu,Y.S., Sack,J.S., Greenhough,T.J., Bugg,C.E., Means,A.R. and Cook,W.J. (1985) Three-dimensional structure of calmodulin. *Nature*, **315**, 37–40.

Bennett,M., Calakos,N. and Scheller,R.H. (1992) Syntaxin: a synaptic protein implicated in docking of synaptic vesicles at presynaptic active zones. *Science*, **257**, 255–259.

Bloembergen,N. (1957) Proton relaxation times in paramagnetic solutions. *J. Chem. Phys.*, **27**, 572–573.

Bodenhausen,G. and Ruben,D.J. (1980) Natural abundance nitrogen-15 NMR by enhanced heteronuclear spectroscopy. *Chem. Phys. Lett.*, **69**, 185–199.

Bommert,K., Charlton,M.P., DeBello,W.M., Chin,G.J., Betz,H. and Augustine,G.J. (1993) Inhibition of neurotransmitter release by C2-domain peptides implicates synaptotagmin in exocytosis. *Nature*, **363**, 163–165.

Brose,N., Petrenko,A.G., Südhof,T.C. and Jahn,R. (1992) Synaptotagmin: a calcium sensor on the synaptic vesicle surface. *Science*, **256**, 1021–1025.

Brose,N., Hofmann,K., Hata,Y. and Südhof,T.C. (1995) Mammalian homologues of *Caenorhabditis elegans unc-13* gene define novel family of C_2-domain proteins. *J. Biol. Chem.*, **270**, 25273–25280.

Davis,D.G. and Bax,A. (1985) Assignment of complex ^1H NMR spectra via two-dimensional homonuclear Hartmann–Hahn spectroscopy. *J. Am. Chem. Soc.*, **107**, 2820–2821.

Davletov,B.A. and Südhof,T.C. (1993) A single C_2 domain from synaptotagmin I is sufficient for high affinity Ca^{2+}/phospholipid binding. *J. Biol. Chem.*, **268**, 26386–26390.

DiAntonio,A. and Schwarz,T.L. (1994) The effect on synaptic physiology of synaptotagmin mutations in *Drosophila*. *Neuron*, **12**, 909–920.

Elferink,L.A., Peterson,M.R. and Scheller,R.H. (1993) A role for synaptotagmin (p65) in regulated exocytosis. *Cell*, **72**, 153–159.

Essen,L.-O., Perisic,O., Cheung,R., Katan,M. and Williams,R.L. (1996) Crystal structure of a mammalian phosphoinositide-specific phospholipase Cδ. *Nature*, **380**, 595–602.

Essen,L.-O., Perisic,O., Lynch,D.E., Katan,M. and Williams,R.L. (1997) A ternary metal binding site in the C_2 domain of phosphoinositide-specific phospholipase C-δ1. *Biochemistry*, **36**, 2753–2762.

Geppert,M., Goda,Y., Hammer,R.E., Li,C., Rosahl,T.W., Stevens,C.F. and Südhof,T.C. (1994) Synaptotagmin I: a major Ca^{2+} sensor for transmitter release at a central synapse. *Cell*, **79**, 717–727.

Grobler,J.A., Essen,L.O., Williams,R.L. and Hurley,J.H. (1996) C2 domain conformational changes in phospholipase C-δ1. *Nature Struct. Biol.*, **3**, 788–795.

Hata,Y., Davletov,B., Petrenko,A.G., Jahn,R. and Südhof,T.C. (1993) Interaction of synaptotagmin with the cytoplasmic domains of neurexins. *Neuron*, **10**, 307–315.

Heidelberger,R., Heinemann,C., Neher,E. and Mathews,G. (1994) Calcium dependence of the rate of exocytosis in a synaptic terminal. *Nature*, **371**, 513–515.

Kee,Y. and Scheller,R.H. (1996) Localization of synaptotagmin-binding domains on syntaxin. *J. Neurosci.*, **16**, 1975–1981.

Li,C., Ullrich,B., Zhang,J.Z., Anderson,G.W., Brose,N. and Südhof,T.C. (1995) Ca^{2+}-dependent and -independent activities of neural and non-neural synaptotagmins. *Nature*, **375**, 594–599.

Lin,J., Abeygunawardana,C., Frick,D.N., Bessman,M.J. and Mildvan,A.S. (1996) The role of Glu57 in the mechanism of the *Escherichia coli* MutT enzyme by mutagenesis and heteronuclear NMR. *Biochemistry*, **35**, 6715–6726.

Littleton,J.T., Stern,M., Schulze,K., Perin,M. and Bellen,H.J. (1993) Mutational analysis of *Drosophila* synaptotagmin demonstrates its essential role in Ca^{2+}-activated neurotransmitter release. *Cell*, **74**, 1125–1134.

Marion,D., Kay,L.E., Sparks,S.W., Torchia,D.A. and Bax,A. (1989) Three-dimensional heteronuclear NMR of ^{15}N-labeled proteins. *J. Am. Chem. Soc.*, **111**, 1515–1517.

Mildvan,A.S. and Cohn,M. (1970) Aspects of enzyme mechanisms studied by nuclear spin relaxation induced by paramagnetic probes. *Adv. Enzymol. Relat. Areas Mol. Biol.*, **33**, 1–70.

Nagar,B., Overduin,M., Ikura,M. and Rini,J.M. (1996) Structural basis of calcium-induced E-cadherin rigidification and dimerization. *Nature*, **380**, 360–364.

Nalefski,E.A. and Falke,J.J. (1996) The C2 domain calcium-binding motif: structural and functional diversity. *Protein Sci.*, **5**, 2375–2390.

Nalefski,E.A., Slazas,M.M. and Falke,J.J. (1997) Ca^{2+}-signaling cycle of a membrane-docking C2 domain. *Biochemistry*, **36**, 12011–12018.

Nicholls,A., Sharp,K.A. and Honig,B. (1991) Protein folding and association: insights from the interfacial and thermodynamic properties of hydrocarbons. *Proteins*, **11**, 281–296.

Nonet,M.L., Grundahl,K., Meyer,B.J. and Rand,J.B. (1993) Synaptic function is impaired but not eliminated in *C.elegans* mutants lacking synaptotagmin. *Cell*, **73**, 1291–1305.

Perin,M.S., Fried,V.A., Mignery,G.A., Jahn,R. and Südhof,T.C. (1990) Phospholipid binding by a synaptic vesicle protein homologous to the regulatory region of protein kinase C. *Nature*, **345**, 260–263.

Perin,M.S., Johnston,P.A., Özcelik,T., Jahn,R., Francke,U. and Südhof,T.C. (1991a) Structural and functional conservation of synaptotagmin (p65) in *Drosophila* and humans. *J. Biol. Chem.*, **266**, 615–622.

Perin,M.S., Brose,N., Jahn,R. and Südhof,T.C. (1991b) Domain structure of synaptotagmin (p65). *J. Biol. Chem.*, **266**, 623–629.

Perisic,O., Fong,S., Lynch,D.E., Bycroft,M. and Williams,R.L. (1998) Crystal structure of a calcium–phospholipid binding domain from cytosolic phospholipase A2. *J. Biol. Chem.*, **273**, 1596–1604.

Petrenko,A.G., Perin,M.S., Davletov,B.A., Ushkaryov,Y.A., Geppert,M. and Südhof,T.C. (1991) Binding of synaptotagmin to the alpha-latrotoxin receptor implicates both in synaptic vesicle exocytosis. *Nature*, **353**, 65–68.

Rizo,J. and Südhof,T.C. (1998) C_2-domains, a novel class of universal Ca^{2+}-binding domains. *J. Biol. Chem.*, **273**, 15879–15882.

Scheller,R.H. (1995) Membrane trafficking in the presynaptic nerve terminal. *Neuron*, **14**, 893–897.

Shao,X., Davletov,B.A., Sutton,R.B., Südhof,T.C. and Rizo,J. (1996) A bipartite Ca^{2+}-binding motif in C_2-domains of synaptotagmin and protein kinase C. *Science*, **273**, 248–251.

Shao,X., Li,C., Fernandez,I., Zhang,X., Südhof,T.C. and Rizo,J. (1997a) Synaptotagmin–syntaxin interaction: the C_2-domain as a Ca^{2+}-dependent electrostatic switch. *Neuron*, **18**, 133–142.

Shao,X., Südhof,T.C. and Rizo,J. (1997b) Assignment of the ^1H, ^{15}N and ^{13}C resonances of the calcium-free and calcium-bound forms of the first C_2-domain of synaptotagmin I. *J. Biomol. NMR*, **10**, 307–308.

Südhof,T.C. (1995) The synaptic vesicle cycle: a cascade of protein–protein interactions. *Nature*, **375**, 645–653.

Südhof,T.C. and Rizo,J. (1996) Synaptotagmins: C_2-domain proteins that regulate membrane traffic. *Neuron*, **17**, 379–388.

Sutton,R.B., Davletov,B.A., Berghuis,A.M., Südhof,T.C. and Sprang,S.R. (1995) Structure of the first C_2 domain of synaptotagmin I: a novel Ca^{2+}/phospholipid-binding fold. *Cell*, **80**, 929–938.

Uellner,R., Zvelebil,M.J., Hopkins,J., Jones,J., MacDougall,L.K., Morgan,B.P., Podack,E., Waterfield,M.D. and Griffiths,G.M. (1997) Perforin is activated by a proteolytic cleavage during biosynthesis which reveals a phospholipid-binding C_2 domain. *EMBO J.*, **16**, 7287–7296.

Yoshida,A., Chikara,O., Omori,A., Kuwahara,R., Ito,T. and Takahashi,M. (1992) HPC-1 is associated with synaptotagmin and ω-conotoxin receptor. *J. Biol. Chem.*, **267**, 24925–24928.

Zhang,O., Kay,L.E., Olivier,J.P. and Forman-Kay,J.D. (1994) Backbone ^1H and ^{15}N assignments of the N-terminal SH3 domain of drk in folded and unfolded states using enhanced-sensitivity pulsed field gradient NMR techniques. *J. Biomol. NMR*, **4**, 845–858.

Zhang,X., Rizo,J. and Südhof,T.C. (1998) Mechanism of phospholipid binding by the C_2A-domain of synaptotagmin I. *Biochemistry*, in press.

Received March 5, 1998; accepted May 7, 1998